Journal of Physiology (1991), **443**, *pp.* 25–44
With 9 figures
Printed in Great Britain

THE EFFECT OF PERMEANT IONS ON SINGLE CALCIUM CHANNEL ACTIVATION IN MOUSE NEUROBLASTOMA CELLS: ION–CHANNEL INTERACTION

BY YAROSLAV M. SHUBA*, VICTOR I. TESLENKO†, ALEXEY N. SAVCHENKO* AND NELLY H. POGORELAYA*

*From the *A. A. Bogomoletz Institute of Physiology, Academy of Sciences of the Ukrainian SSR, Kiev, USSR and the †Institute for Theoretical Physics, Academy of Sciences of the Ukrainian SSR, Kiev, USSR*

(*Received 19 October 1990*)

SUMMARY

1. Single low-threshold inactivating (LTI or T-type) Ca^{2+} channels of undifferentiated neuroblastoma cells (clone N1E-115) were investigated using the patch-clamp technique.

2. Single-channel conductance, g_i, for Ca^{2+}, Sr^{2+} or Ba^{2+} as a permeant cation was similar (7·2 pS). Mean channel open time , τ_{op}, was also practically independent of the divalent ion species; it decreased from 0·7 to 0·3 ms between −40 and 0 mV.

3. Modification of the calcium channel selectivity by lowering the external Ca^{2+} concentration to 10^{-8} M produced an increase in g_i for Na^+ and Li^+ ions and a shift of potential-dependent characteristics in the hyperpolarizing direction. Voltage sensitivity and absolute values of τ_{op} were also changed. These changes were dependent on both permeant monovalent ion type and concentration.

4. At high $[Na^+]_o$, τ_{op} was almost potential independent ($\simeq$ 0·3 ms). Decrease in $[Na^+]_o$ and substitution of Li^+ for Na^+ increased τ_{op} and the steepness of its potential dependency.

5. The divalent and monovalent cations that were tested had much smaller effect on the mean intraburst shut time, $\tau_{cl(f)}$, which was nearly independent of membrane potential ($\simeq$ 0·6 ms). By contrast, mean burst duration was strongly potential dependent and noticeably affected by permeant ion type.

6. All kinetic changes were analysed in terms of a four-state sequential model for channel activation. According to this model the channel enters the open state through three closed states. Transitions between closed states can be formally related to the transmembrane movement of two charged gating particles (m^2 process). The interaction between ion flux and a sterical region of the Ca^{2+} channel selectivity filter may, depending on ion transfer rate and ionic radius, lead to a local increase of the dielectric constant, resulting in redistribution of the electric field and changes in potential dependency of τ_{op}.

MS 8874

INTRODUCTION

In previous investigations of Ca^{2+} channel selectivity and gating at the whole-cell level, it has been shown that the inactivation time course of current is strongly affected by permeant ion species and concentration (Tillotson, 1979; Ashcroft & Stanfield, 1981; Brown, Morimoto, Tsuda & Wilson, 1981; Eckert & Tillotson, 1981; Ganitkevich, Shuba & Smirnov, 1987). This effect, however, has most often been explained by the involvement of Ca^{2+}-dependent inactivation mediated through the cellular metabolic pathways rather than by direct ion–channel interaction (e.g. Chad & Eckert, 1986). The whole-cell data concerning the effect of permeating ions on Ca^{2+} channel activation and deactivation ('tail' current) are contradictory. Some authors have reported that there is no obvious effect of permeant ions on Ca^{2+} channel activation–relaxation kinetics (Hagiwara, Ozawa & Sand, 1975; Byerly & Hagiwara, 1982; Fox, Nowycky & Tsien, 1987*a*; Carbone & Lux, 1988) while others have noted distinct changes (Fenwick, Marty & Neher, 1982; Siami & Kung, 1982; Brown, Tsuda & Wilson, 1983; McDonald, Cavalie, Trautwein & Pelzer, 1986; Kostyuk & Shirokov, 1989). Although this disagreement is likely, in part, to be due to tissue specificity of Ca^{2+} channels, it is our view that the whole-cell experiments do not allow adequate resolution of all kinetic stages of the activation process (Kostyuk, Shuba & Teslenko, 1989*b*). Indeed, in almost all studies carried out at the single Ca^{2+} channel level, an effect of permeant ions on mean open time has been detected (Cavalie, Ochi, Pelzer & Trautwein, 1983; Nelson, 1986; Carbone & Lux, 1987*b*). However, a detailed investigation is still required, especially one to relate the changes in Ca^{2+} channel gating to a definite kinetic model of its activation.

It is well established that the Ca^{2+} permeability of the neuronal membrane is due to the activity of two (Veselovsky & Fedulova, 1983; Carbone & Lux, 1984; Fedulova, Kostyuk & Veselovsky, 1985) or possibly three (Nowycky, Fox & Tsien, 1985; Fox *et al.* 1987*a*, *b*; Kostyuk, Shuba & Savchenko, 1988*a*) types of potential-dependent Ca^{2+} channels differing in their voltage dependence, kinetics, selectivity and pharmacology. We have found that undifferentiated neuroblastoma cells (clone N1E-115) possess Ca^{2+} channels which have properties very similar to low-threshold inactivating (LTI) Ca^{2+} channels of vertebrate sensory neurones. In the present investigation the properties of these unitary LTI Ca^{2+} channels were studied using the patch-clamp technique. The changes in channel gating due to substitution of different permeant divalent and monovalent ions were analysed in terms of a four-state sequential model for channel activation (Kostyuk *et al.* 1989*b*). Monovalent ion permeability was induced by lowering the external Ca^{2+} concentration to 10^{-8} M (Kostyuk, Mironov & Shuba, 1983; Almers, McCleskey & Palade, 1984; Fukushima & Hagiwara, 1985; Hess, Lansman & Tsien, 1986; Carbone & Lux, 1987*b*). LTI Ca^{2+} channels are especially convenient for the study of ion–channel interaction because they do not reveal Ca^{2+}-dependent inactivation and are independent from intracellular metabolic support (Carbone & Lux, 1984, 1987*b*; Quandt & Narahashi, 1984; Fedulova *et al.* 1985; Kostyuk *et al.* 1988*a*). This allows us to exclude any indirect action of permeant ions on channel gating.

Preliminary results have been presented (Kostyuk, Shuba, Savchenko & Teslenko, 1988*b*; Kostyuk, Akaike, Osipchuk, Savchenko & Shuba, 1989*a*).

METHODS

Preparation. Mouse neuroblastoma cells (clone N1E-115, line C 1300) were cultured on cover-slips placed in Petri dishes filled with DMEM cultured medium (Serva) supplied with glucose (4·5 g/l) and 10% of fetal calf serum.

Electrophysiology and solutions. Experiments were carried out using the patch-clamp technique (Hamill, Marty, Neher, Sakmann & Sigworth, 1981). Macroscopic currents were recorded in the whole-cell configuration. In this case the external solution contained either Ca^{2+}, Sr^{2+} or Ba^{2+} as a charge carrier and had the following composition (mM): $CaCl_2$ ($SrCl_2$ or $BaCl_2$), 15; $MgCl_2$, 4; tetraethylammonium chloride (TEA-Cl), 110; HEPES, 10; tetrodotoxin (TTX), 10^{-3}. The pH was adjusted to 7·3 by NaOH. The recording pipette was filled with intracellular saline containing (mM): CsCl, 60; caesium aspartate, 60; Cs-EGTA, 10; HEPES, 20; $MgCl_2$, 4; pH 7·2. Analog compensation of leakage current was used when recording whole-cell current.

Single-channel recording was performed mostly in the cell-attached configuration. The resting potential (V_r) was brought to zero by using an extracellular solution containing a high concentration of K^+ (mM): potassium aspartate, 140; K-EGTA, 10; HEPES, 20; $MgCl_2$, 5; pH 7·3. During single Ca^{2+} channel recording either 60 mM-Ca^{2+}, Sr^{2+} or Ba^{2+} was presented in the pipette solution as permeant cation; 2 mM-$MgCl_2$, 40 mM-TEA-Cl, 10 mM-HEPES and 10^{-6} M-TTX were also added and the pH was titrated to 7·3 with NaOH. When recording the activity of single Ca^{2+} channels with modified selectivity, the free Ca^{2+} concentration in the pipette solution was buffered to 10^{-8} M. At this concentration Ca^{2+} ions have no effect on the function of modified single Ca^{2+} channels (Carbone & Lux, 1987*b*). Na^+ and Li^+ ions at various concentrations were used as charge carriers through the modified Ca^{2+} channels. The basic composition of the pipette solution was as follows (mM): NaCl, 60; TEA-Cl, 85; $CaCl_2$, 0·91; EGTA, 10; TTX, 10^{-3}; HEPES, 10; pH 7·3. The changes in permeant ion concentration were made in parallel with equimolar changes in TEA-Cl concentration. All experiments were carried out at room temperature (20–22 °C).

Data analysis. Single-channel currents were low-pass filtered at 1 or 2 kHz and digitized at a frequency of 10 kHz. Capacitative and leakage currents were eliminated by subtracting from each record the average of records without channel activity. Half-amplitude threshold was used for detection of channel openings and closings. With such a threshold, the 'dead time', t_d (maximum pulse duration in which current amplitude does not reach the threshold), is related to the corresponding bandwidth, Δf, as $t_d = 0{\cdot}183/\Delta f$ (Colquhoun & Sigworth, 1983). Standard deviation of background noise fluctuations, σ_n, was about 0·05 pA at $\Delta f = 1$ kHz increasing to $\simeq$ 0·08 pA at $\Delta f = 2$ kHz. Unitary current amplitude, A_0, for divalent charge carriers decreased from 0·66 to 0·26 pA in the range of membrane potentials -50 to 0 mV. This means that the relative threshold, $A_0/2\sigma_n$, is about 6 at a membrane potential $V_m = -50$ mV and only 2·5 at $V_m = 0$ mV. Thus, the rate of detection of false events, λ_f, increases with the depolarization in this potential range from about 10^{-4} s^{-1} to 50 s^{-1} (Colquhoun & Sigworth, 1983). For the Na^+ current through the modified Ca^{2+} channels at $[Na^+]_o = 40$ mM and $V_m = -40$ mV (worst case), $A_0/2\sigma_n$ is of the order of 2·5 and $\lambda_f \simeq 50$ s^{-1}. Distortions of measured time constants related to false openings of short duration were avoided by excluding the initial part (0·2 ms) of open time and burst duration histograms from the fitting procedure.

For the experimental conditions when the highest rate of false openings occurred ($\lambda_f \simeq 50$ s^{-1}) an additional closed period longer than 20 ms might contribute to the closed time and first latency histograms. However, it was not difficult to distinguish these periods from real closings since they were distributed randomly and their duration was 2–3 times longer than the 'very slow' ($\tau_{cl(vs)}$) time constant of these histograms (see Table 1). So, by choosing of the appropriate part of closed time and first latency histograms for the fitting procedure it was possible to take into account all real channel closings and to neglect false ones.

Using half-amplitude threshold, original records were idealized. Idealized records were used for construction of averaged currents and time histograms. To identify bursts, all shut intervals which were equal to or less than three times the mean duration of the 'fastest' component of the closed time histogram ($\tau_{cl(f)}$) were considered to be gaps within bursts (Magleby & Pallota, 1983).

I–V relations of unitary Ca^{2+} channel for monovalent permeant cations were constructed from responses of membrane patches stimulated with voltage ramps. Discrete open channel amplitudes obtained from ramp records were averaged and represented in *I–V* co-ordinates after digital filtering to reduce noise.

RESULTS

Divalent charge carriers

With 15 mM-Ca^{2+}, Sr^{2+} or Ba^{2+} in the external Na^+, K^+-free solution the depolarization of the neuroblastoma cell membrane from a holding potential (V_h) of −90 mV evoked an inward-going whole-cell current that was activated at $V_m = -60$ to −40 mV (Fig. 1*A*). With increasing depolarization, current amplitude increased

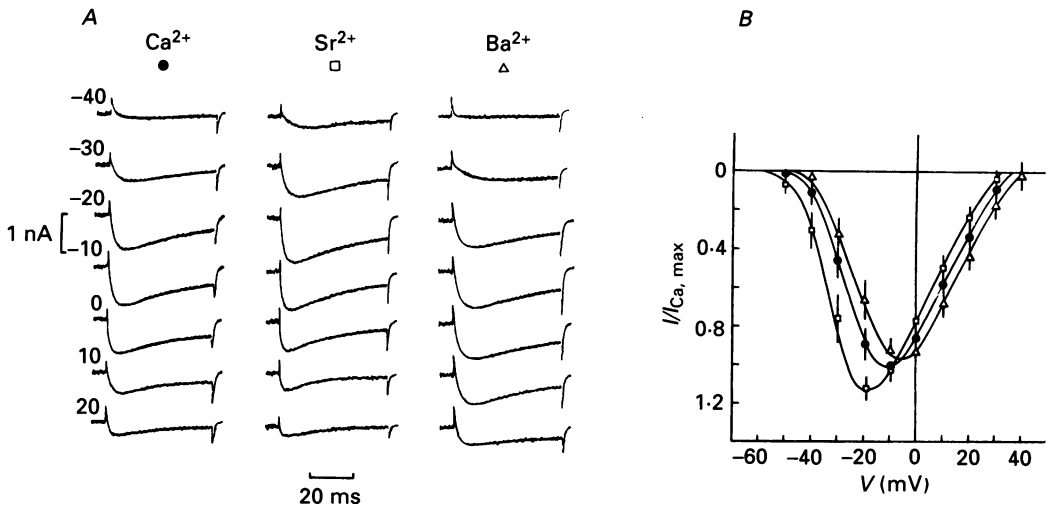

Fig. 1. Whole-cell currents through Ca^{2+} channels of neuroblastoma cells for divalent charge carriers, Ca^{2+}, Sr^{2+} and Ba^{2+}, all at 15 mM. *A*, original current records for indicated membrane potentials (mV). *B*, averaged *I–V* relations (mean ± S.D. from seven cells normalized to the maximum Ca^{2+} current $I_{Ca,max}$).

and reached its maximum at $V_m = -20$ to 0 mV. At higher depolarizations, current decreased again. The apparent reversal was observed at $V_m = +30$ to +40 mV (Fig. 1*B*). Since the composition of the external and internal solutions ensured that other permeabilities were suppressed, these currents were attributed to the activation of Ca^{2+} channels. In contrast to dorsal root ganglion (DRG) neurons (Veselovsky & Fedulova, 1983; Carbone & Lux, 1984, 1987*a*; Fedulova *et al.* 1985) and differentiated neuroblastoma cells (Fishman & Spector, 1981; Narahashi, Tsunoo & Yoshii, 1987) only one component of inward current was observed under our conditions in the range of membrane potentials −90 to +80 mV. This suggests that only one type of potential-operated Ca^{2+} channel occurs in our preparation.

After the onset of depolarization, the current carried by Ca^{2+}, Sr^{2+} and Ba^{2+} ions reached a maximal value and then inactivated with time. The amplitudes of whole-cell currents for different divalent charge carriers were related to each other in the following way: $I_{Ca}:I_{Sr}:I_{Ba} = 1:1{\cdot}12:0{\cdot}94$ (Fig. 1*B*). This sequence differs from that usually found for high-threshold Ca^{2+} channel currents in a large variety of preparations which has the highest amplitude in Ba^{2+}-containing solution and decreases after substitution of Sr^{2+} or Ca^{2+} for Ba^{2+} (Bean, 1985; Bossu, Feltz &

Thomann, 1985; Fedulova *et al.* 1985; Matteson & Armstrong, 1986; Carbone & Lux, 1987*a*; Fox *et al.* 1987*a*). On the other hand, a similar sequence to that determined here has been reported for whole-cell currents through LTI Ca^{2+} channels in lymphocytes (Fukushima & Hagiwara, 1985), vertebrate sensory neurons (Bossu *et al.* 1985; Carbone & Lux, 1987*a*, *b*), glomerulosa cells (Durroux, Gallo-Payet & Payet, 1988) and heart cells (Bean, 1985).

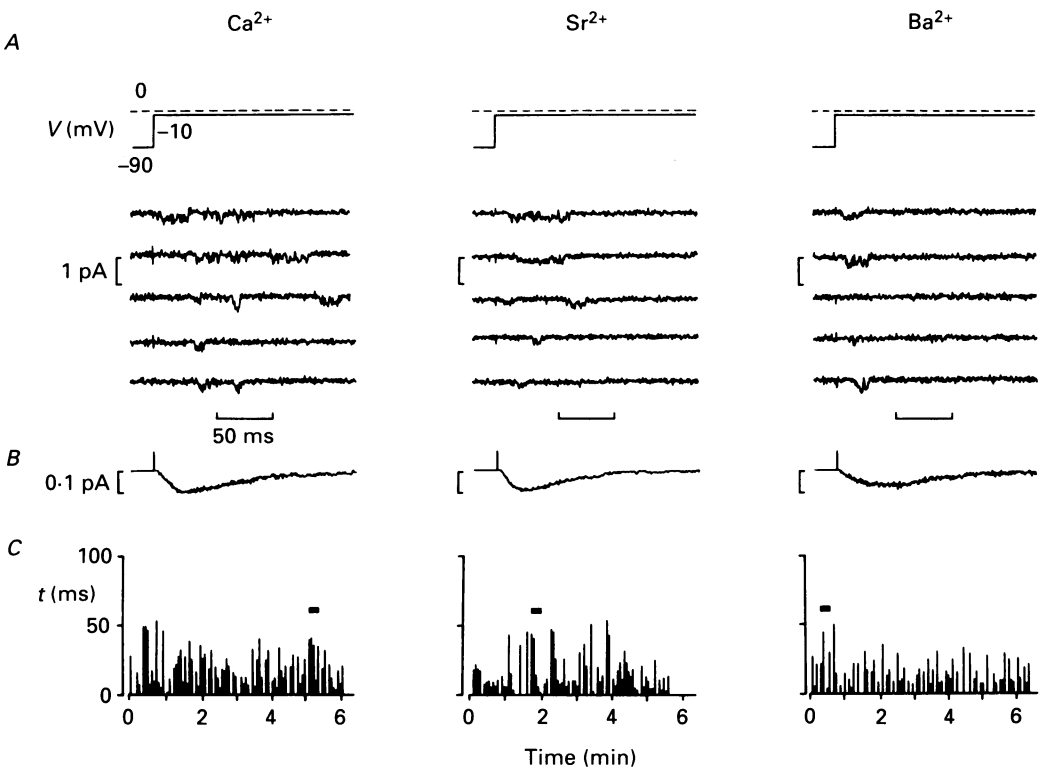

Fig. 2. Single Ca^{2+} channel activity in neuroblastoma cell membrane for divalent charge carriers. *A*, voltage protocols and original current records for Ca^{2+}, Sr^{2+} and Ba^{2+} (60 mM) as charge carriers. Cell-attached configuration, resting membrane potential was zeroed. Recording bandwidth, 1 kHz. *B*, corresponding averages of computer-idealized current records. *C*, changes in total channel open time *t* in response to consecutive depolarization of 400 ms duration at 0·25 Hz (height of the columns) during the course of the experiment. Horizontal bars indicate records shown in *A*.

The *I–V* relation of the whole-cell current was shifted by permeant divalent cations along the voltage axis in the depolarizing direction (measured as a change in the potential of half-maximal current, $V_{\frac{1}{2}}$) according to the sequence $Ba^{2+} > Ca^{2+} > Sr^{2+}$. This sequence is also quite similar to that reported for LTI current in other preparations ($Ba^{2+} \simeq Ca^{2+} > Sr^{2+}$; Bean, 1985; Fukushima & Hagiwara, 1985), but different from that for high-threshold current ($Ca^{2+} > Sr^{2+} > Ba^{2+}$; Fedulova *et al.* 1985). We also found a difference in apparent reversal potential of the corresponding currents. This was, however, almost the same as the $V_{\frac{1}{2}}$. That is why we would not

attribute shifts of reversal potential to different permeabilities for the divalent cations.

Figure 2*A* shows single Ca^{2+} channel currents for divalent charge carriers. Ensemble averages varied in amplitude as the corresponding whole-cell currents (Fig. 2*B*), although unitary current amplitudes in Ca^{2+}, Sr^{2+} and Ba^{2+} solutions were practically identical (Fig. 3*D*) as were channel slope conductances (7·2 pS). In

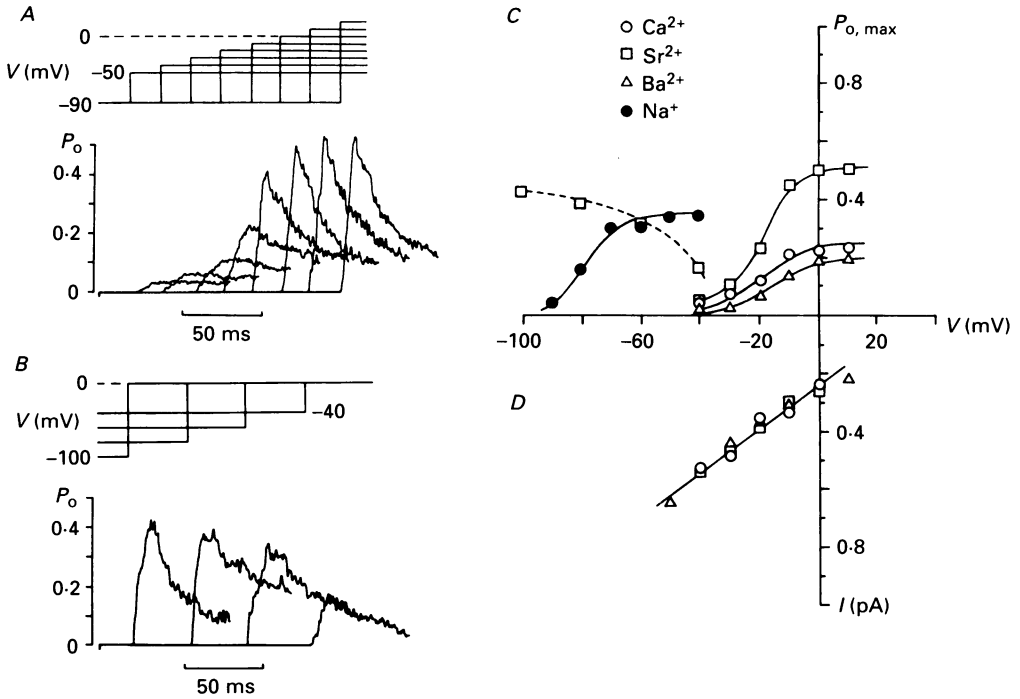

Fig. 3. Stationary characteristics of single Ca^{2+} channel of neuroblastoma cells. *A*, the probability of the channel being open, P_o, as a function of time for various test potentials from holding potential −90 mV (60 mM-Sr^{2+}). *B*, the same as *A* but in response to variation of holding potential at a fixed test potential (0 mV). Each P_o curve was generated using 80–120 single-channel records for corresponding potentials with subsequent averaging of the data from three to five patches. Voltage protocols are shown at the top of *A* and *B*. *C*, Ca^{2+} channel activation curves (maximal P_o, $P_{o,max}$ as a function of membrane potential) for Ca^{2+}, Sr^{2+}, Ba^{2+} and Na^+ (60 mM). Dashed line indicates the curve of steady-state inactivation (60 mM-Sr^{2+}). *D*, Ca^{2+} channel *I–V* relations for different divalent charge carriers (60 mM); conductance, 7·2 pS. Different symbols in *C* and *D* indicate mean experimental values for corresponding charge carriers; continuous lines are the best fit by eye.

addition, there was no significant change in the total channel open time t during successive depolarizations when one permeant ion was substituted for another (Fig. 2*c*). However, there were more blank records when Ba^{2+} was used as a charge carrier compared to Ca^{2+} or Sr^{2+}. As a result, averaged currents revealed variation in amplitude, and activation curves of the channel for Ba^{2+}, Ca^{2+} and Sr^{2+} had different saturation levels of 0·2, 0·3 and 0·5, respectively. The observed relative shifts of

channel activation curves by different permeant ions were in qualitative agreement with those for *I–V* relations of the corresponding whole-cell currents (Fig. 3*C*).

During single-channel recording with divalent charge carriers the V_h was set at −90 mV. Shifting V_h in the depolarizing direction caused stationary inactivation of the channel (Fig. 3*B* and *C*). Half-inactivation was observed at about −40 mV for Sr^{2+} as a permeant cation.

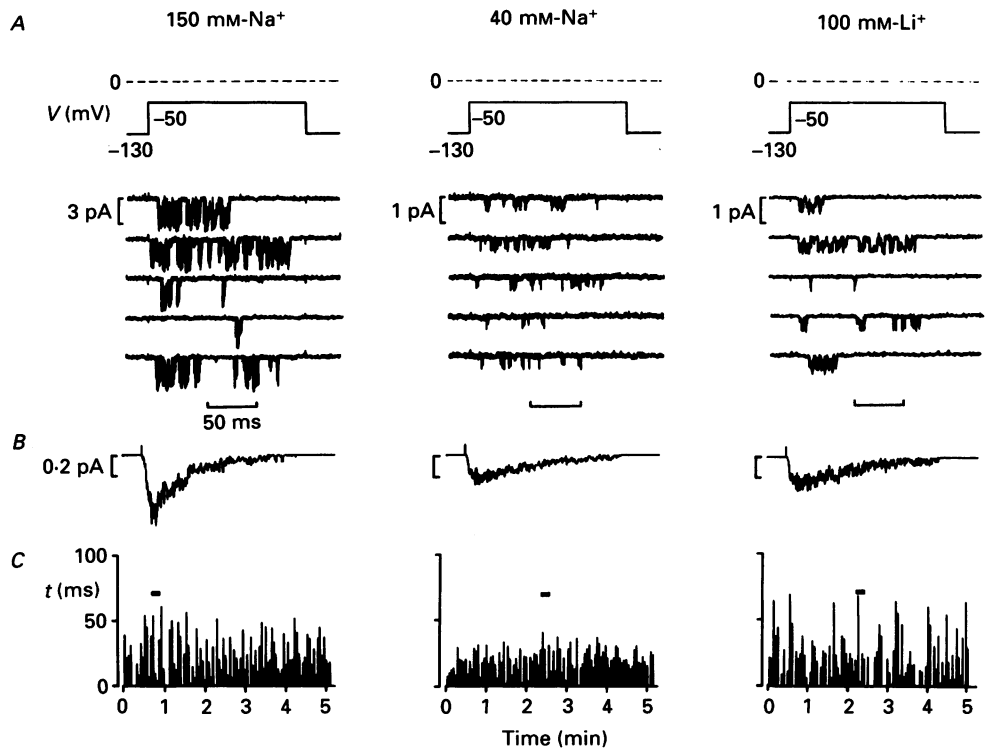

Fig. 4. Activity of modified Ca^{2+} channel of neuroblastoma cells. Na^+ (150 and 40 mM) and Li^+ (100 mM) as charge carriers. Recording bandwidth 2 (Na^+) and 1 (Li^+) kHz. Details as in Fig. 2.

Monovalent charge carriers

Figure 4 shows examples of single-channel activity in neuroblastoma cell membrane after a decrease in external Ca^{2+} concentration to 10^{-8} M. Na^+ and Li^+ were used as charge carriers. Since there are no TTX-resistant Na^+ channels in neuroblastoma cells (Moolenaar & Spector, 1978; Fishman & Spector, 1981; Quandt & Narahashi, 1984; Narahashi *et al.* 1987), we attributed this activity to single Ca^{2+} channels with modified selectivity. The main features of modified Ca^{2+} channels were a strong increase in the conductance and a substantial shift of the activation characteristic in the hyperpolarizing direction (~ 70 mV, Fig. 3*C*). The *I–V* relations of modified Ca^{2+} channels obtained from ramp records for Na^+ concentrations in the range of 40–150 mM and Li^+ at 100 mM are presented in Fig. 5. Under our experimental conditions when total current through the modified Ca^{2+} channel

consisted of inward Na^+ or Li^+ and outward K^+ currents, all I–V relations were linear up to $V_m = +30$ mV, and channel conductances for 40, 60, 100 and 150 mM-Na^+ and 100 mM-Li^+ were 10, 18, 32 and 57 pS and 11 pS, respectively. In contrast to observations by Hess *et al.* (1986) on single high-threshold non-inactivating (HTN or

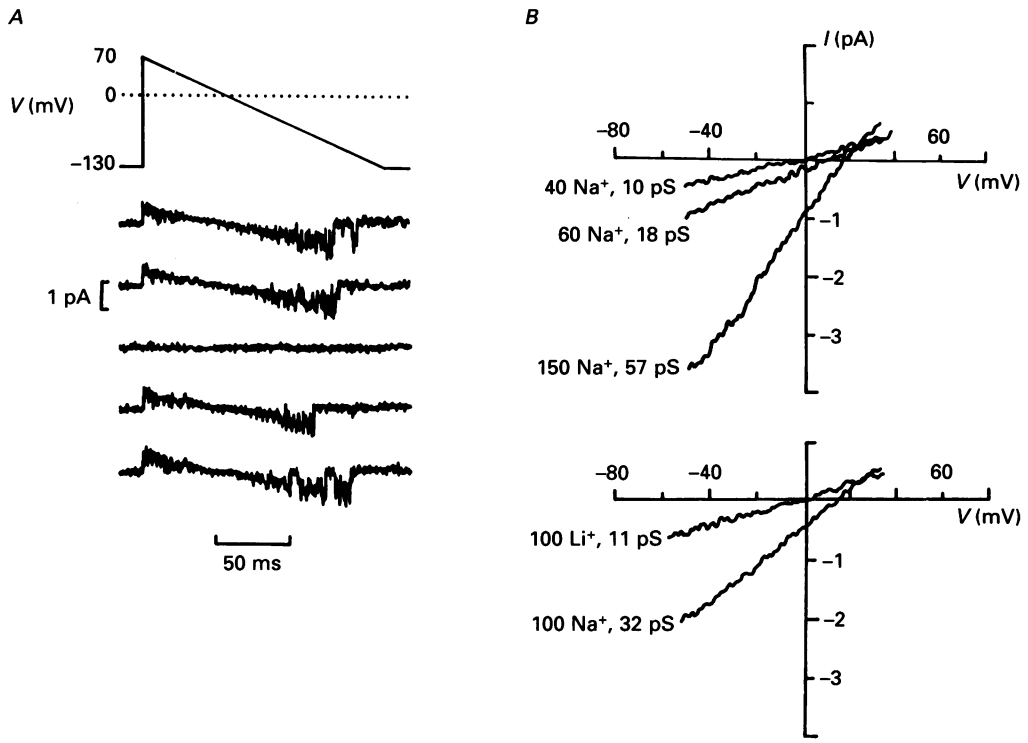

Fig. 5. Ramp recordings of modified Ca^{2+} channel. *A*, voltage protocol and original current records (60 mM-Na^+ as a charge carrier). *B*, modified Ca^{2+} channel I–V relations obtained after averaging of discrete channel openings from ramp recordings and digital filtering of resultant curves to reduce noise (corresponding concentrations (mM) and conductance of charge carriers are shown near each curve).

L-type) Ca^{2+} channels of guinea-pig ventricular myocytes, we could detect clear unitary outward current at depolarizations to potentials more positive than the reversal potential. However, at V_m higher than +40 mV multiple unitary events appeared relatively frequently. They could arise from the presence of more than one Ca^{2+} channel in the patch since rare superimpositions were observed also at more negative V_m. A contribution of K^+ channels to the unitary outward currents seems to be improbable since in most cases the pipette solution contained relatively high concentrations of TEA (except in $[Na^+]_o = 150$ mM) and only less than 10% of all patches contained channel activity consisting of outward currents without accompanying inward currents. For the construction of I–V relations, we tried to choose only those ramp records which did not contain apparent overlapping events. Nevertheless, we are uncertain of current values at membrane potentials more positive than +30 to +40 mV.

The sequence of relative permeabilities for monovalent cations was obtained by using the following expressions derived from the Goldman–Hodgkin–Katz equation (Hille, 1975):

$$V_{Na} = RT/F \ln (P_{Na}[Na^+]_o/P_K[K^+]_i),$$

$$V_{Na} - V_{Li} = RT/F \ln (P_{Na}[Na^+]_o/P_{Li}[Li^+]_o),$$

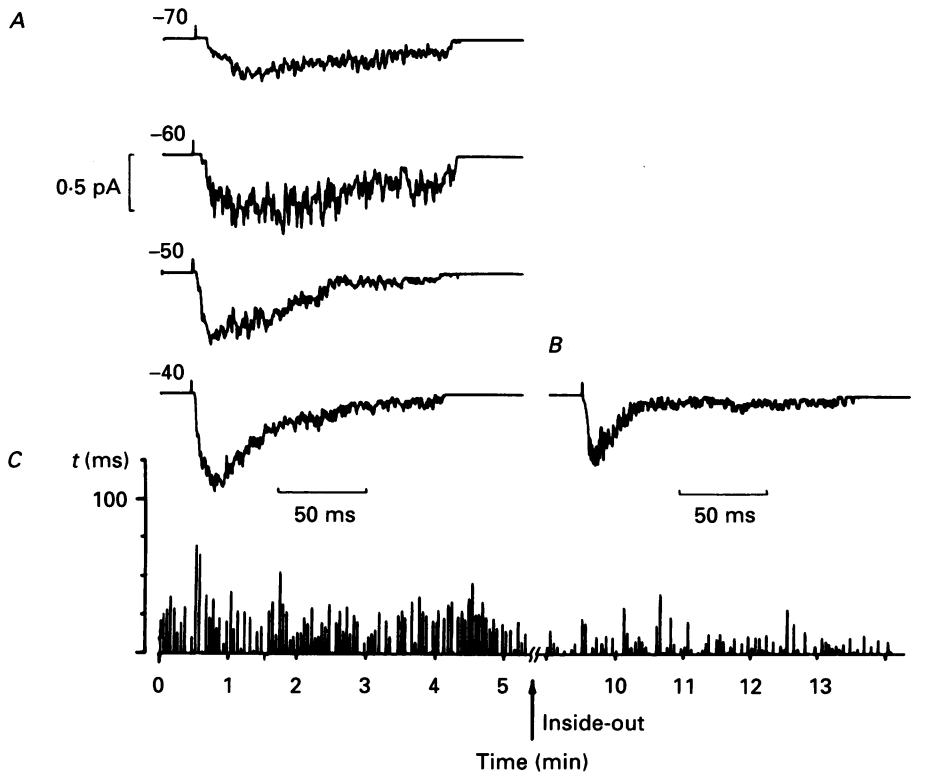

Fig. 6. Effect of patch excision on the activity of modified Ca^{2+} channel of neuroblastoma cells. *A*, averages of computer-idealized single-channel records for indicated membrane potentials (mV) obtained in cell-attached configuration (100 mM-Na^+ as a charge carrier). *B*, the same for a membrane potential of −40 mV after formation of inside-out configuration. *C*, changes of total channel open time *t* in response to consecutive depolarizations during the course of the experiments.

where V_{Na}, V_{Li} are reversal potentials for Na^+ and Li^+ currents, P_{Na}, P_K, P_{Li} are permeabilities, $[Na^+]_o$ and $[Li^+]_o$ are external and $[K^+]_i$ internal ion concentrations, and *R*, *T* and *F* have their usual meanings. For 100 mM $[Na^+]_o$, 100 mM $[Li^+]_o$ and 150 mM $[K^+]_i$, these expressions give: $P_{Na}:P_K:P_{Li} = 1:0{\cdot}35:0{\cdot}55$. It should be mentioned, however, that variations in reversal potential observed in response to changes in external Na^+ and Li^+ concentrations were not in a good agreement with theoretical predictions of the Goldman–Hodgkin–Katz formula. One reason for this may be the deviation of the internal K^+ concentration from 150 mM and its variation for different cells. However, we do not exclude the possibility of a concentration dependence of relative permeabilities for modified LTI Ca^{2+} channels.

The activity of modified Ca^{2+} channels was preserved after excision of the membrane path and formation of the inside-out configuration (Fig. 6). However, the mean current from excised patches had a smaller amplitude due to both a decrease in total channel open time during depolarization and an increase in the number of blank records (Fig. 6). Such reduced activity could be observed for a long time with no sign of run-down.

Ca^{2+} channel activation kinetics

A four-state kinetic model for the description of Ca^{2+} channel activation has recently been proposed (Kostyuk *et al.* 1989*b*):

$$\mathrm{R} \underset{\beta}{\overset{2\alpha}{\rightleftharpoons}} \mathrm{C} \underset{2\beta}{\overset{\alpha}{\rightleftharpoons}} \mathrm{A} \underset{b}{\overset{a}{\rightleftharpoons}} \mathrm{O}, \tag{1}$$

where R, C and A are closed states, O is the open state of the channel and α, β, a and b are the rate constants of channel transitions between the states. In terms of this model an adequate description of all experimental histograms was possible. Formally, the first two stages in model (1) can be attributed to a potential-dependent transfer of two charged gating particles in conformity with m^2 activation kinetics (Kostyuk, Krishtal & Shakhovalov, 1977), while the last kinetic stage describes subsequent fast (perhaps conformational) transformation of the channel gating mechanism which leads directly to channel opening.

The kinetics of Ca^{2+} channels in the neuroblastoma cells under investigation seem to be similar to those of LTI Ca^{2+} channels in neuronal membrane, the activation of which at the whole-cell level can be described using the m^2 Hodgkin–Huxley formalism (Fedulova *et al.* 1985). Thus,it was interesting to test the validity of model (1) for the present case and to examine how different kinetic stages of the channel activation may depend on permeant ion species. Although the model does not consider inactivation, we note that Carbone & Lux (1987*b*) have suggested that Ca^{2+} channels can enter the inactive state from any foregoing state, and we discuss below the possible contribution of this to the measured rate constants.

The validity of model (1) was tested using the data-fitting procedure of Kostyuk *et al.* (1989*b*). The open time histogram could be adequately fitted with a single exponential (Fig. 7*Aa* and *Ba*) with time constant, τ_{op}, which is the inverse of rate constant b ($\tau_{op} = 1/b$). The histogram of channel lifetime in the closed state required at least three exponentials to describe the data (Fig. 7*Ab* and *Bb*). The 'fast' exponential component of this histogram contained the highest fraction of all channel closures, and its time constant, $\tau_{cl(f)}$, characterizes the mean value of intraburst shut times. In the framework of the model (1) this time constant can be expressed as (Shuba & Teslenko, 1987):

$$1/\tau_{cl(f)} \simeq a + 2\beta(1 + \alpha/a) \simeq a + 2\beta. \tag{2}$$

The burst duration histogram could be well approximated by the sum of two exponentials (Fig. 7*Ac* and *Bc*). The time constant of the 'slower' exponential,

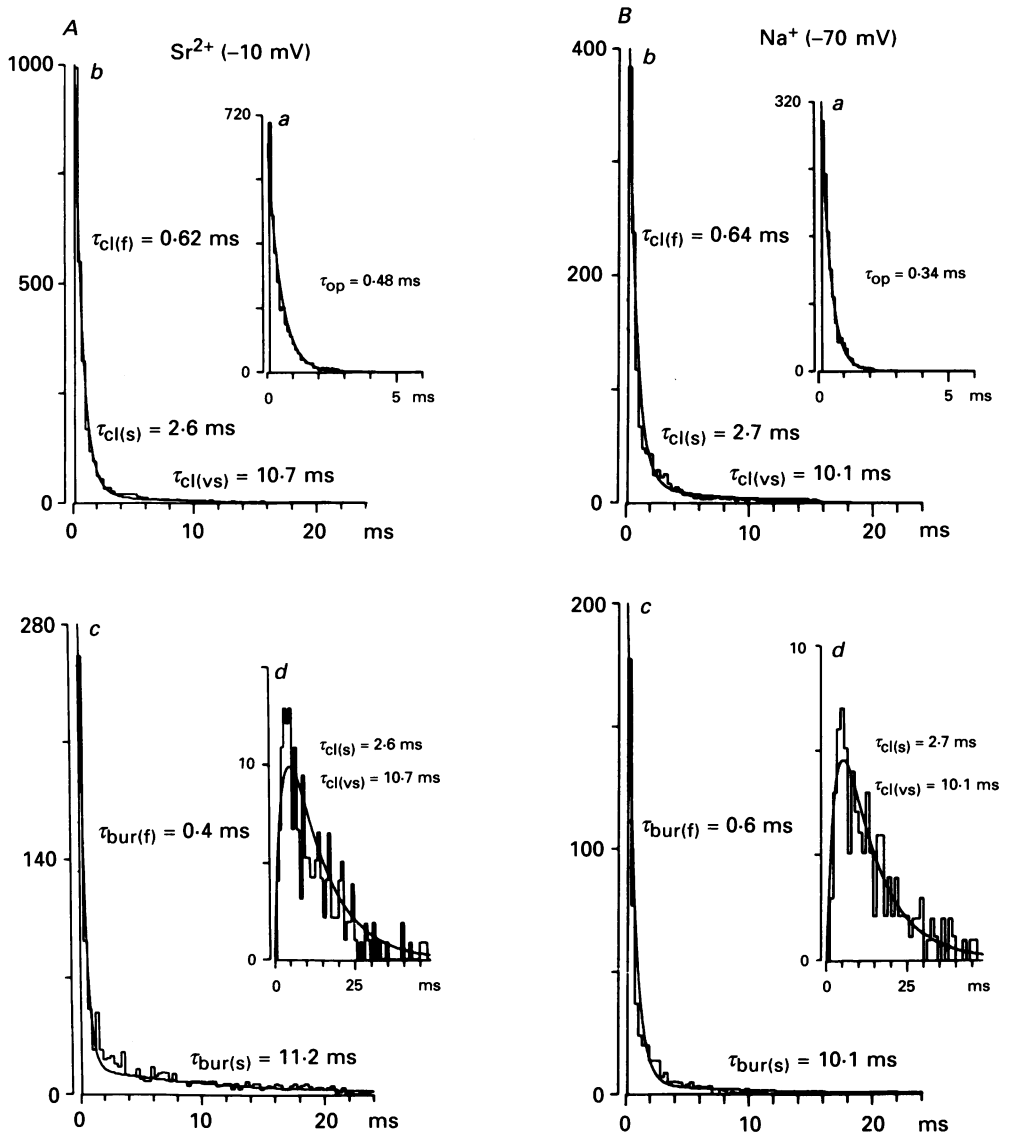

Fig. 7. Fitting of experimental time histograms for single Ca^{2+} channel activity in neuroblastoma cell membrane in conformity to model (1) (see text). Examples of open time (*a*), closed time (*b*), burst duration (*c*) and latency to first opening (*d*) histograms for 60 mM-Sr^{2+} (*A*) and 60 mM-Na^{+} (*B*) as charge carriers. Smooth curves are single- (*a*), three- (*b*) and double- (*c* and *d*) exponential fittings (*b* and *c*, sum; *d*, difference of exponentials) to the experimental histograms. Corresponding time constants are shown near each histogram.

$\tau_{bur(s)}$, is related to the rate constants a, b and β according to the following expression (Shuba & Teslenko, 1987; Kostyuk *et al.* 1989*b*):

$$1/\tau_{bur(s)} \simeq 2b\beta/(a+b). \quad (3)$$

Using eqns (2) and (3) and considering that $b = 1/\tau_{op}$ one can easily obtain the

relations which allow to calculate the rate constants a and β based on experimentally measured τ_{op}, $\tau_{cl(f)}$ and $\tau_{bur(s)}$:

$$a = (\tau_{bur(s)} - \tau_{cl(f)})/\tau_{cl(f)}(\tau_{bur(s)} + \tau_{op}),$$

$$\beta = (\tau_{op} + \tau_{cl(f)})/2\tau_{cl(f)}(\tau_{bur(s)} + \tau_{op}).$$

The histogram of the first latencies to channel opening after depolarization onset could be satisfactorily fitted by the difference of two exponentials (Fig. 7*A d* and *B d*)

TABLE 1. Mean values of inverse rate constants a^{-1}, b^{-1}, α^{-1}, β^{-1} and time constant $\tau_{cl(s)}$ and $\tau_{cl(vs)}$ (in ms) for different permeant ions (all in 60 mM concentration) and different membrane potentials

Ion	V_m (mV)	a^{-1}	b^{-1}	α^{-1}	β^{-1}	$\tau_{cl(s)}$	$\tau_{cl(vs)}$
Ca^{2+}	−30	0·53	0·56	20·3	9·6	4·0	51·6
	−20	0·58	0·54	16·2	10·8	3·8	33·7
	−10	0·50	0·40	9·5	12·5	3·0	15·1
	0	0·44	0·36	7·5	13·8	2·7	10·6
Sr^{2+}	−30	0·54	0·59	16·4	8·6	3·5	39·1
	−20	0·46	0·43	11·7	11·0	3·3	21·0
	−10	0·42	0·36	7·4	13·1	2·6	10·1
	0	0·34	0·29	5·4	16·5	2·2	6·8
Ba^{2+}	−30	0·77	0·62	30·3	6·6	3·7	123·7
	−20	0·53	0·50	18·7	7·6	3·6	49·1
	−10	0·46	0·45	10·8	10·3	3·0	19·2
	0	0·40	0·36	5·8	14·5	2·2	7·6
Na^{+}	−90	0·65	0·40	17·0	8·6	3·7	39·0
	−80	0·67	0·39	11·5	10·7	3·3	20·1
	−70	0·61	0·39	7·4	14·8	2·7	10·1
	−60	0·57	0·37	4·1	19·2	1·8	4·8

having the same time constants as 'slow' ($\tau_{cl(s)}$) and 'very slow' ($\tau_{cl(vs)}$) exponential components of the overall closed time histograms. These time constants allow one to determine the rate constant α using the expression (Kostyuk *et al.* 1989*b*):

$$\alpha = (2\tau_{cl(s)}\tau_{cl(vs)})^{-0.5}.$$

It is necessary to point out that the described procedure of data processing was valid for an adequate description of channel activation irrespective of permeant ion species (see Fig. 7). This allowed us to determine a full set of rate constants describing channel activation in the framework of model (1) for different charge carriers (see Table 1). Figure 8*A* and *B* shows the potential dependence of mean channel open time and mean time of intraburst channel closures for divalent and monovalent charge carriers. The absolute values of these time constants and their potential dependence for Ca^{2+}, Sr^{2+} and Ba^{2+} are very similar. Modification of normal channel selectivity that allowed high permeability to monovalent cations led first of all to a hyperpolarizing shift of $\tau_{op}(V)$ and $\tau_{cl(f)}(V)$ compared to divalent charge carriers. The absolute values of $\tau_{cl(f)}$ for Na^{+} and Li^{+} were almost the same as for Ca^{2+}, Sr^{2+} and Ba^{2+} and varied only slightly with changes in membrane potential. However, τ_{op} showed more prominent variations which depended on both permeant monovalent

ion type and concentration. The potential dependence of the mean channel open time for Na^+ was much weaker, and absolute values smaller, than for Li^+ and divalent charge carriers. Values for τ_{op} also depended on Na^+ concentration, being smaller for 100 mM $[Na^+]_o$ than for 40 mM $[Na^+]_o$ (Fig. 8*A*).

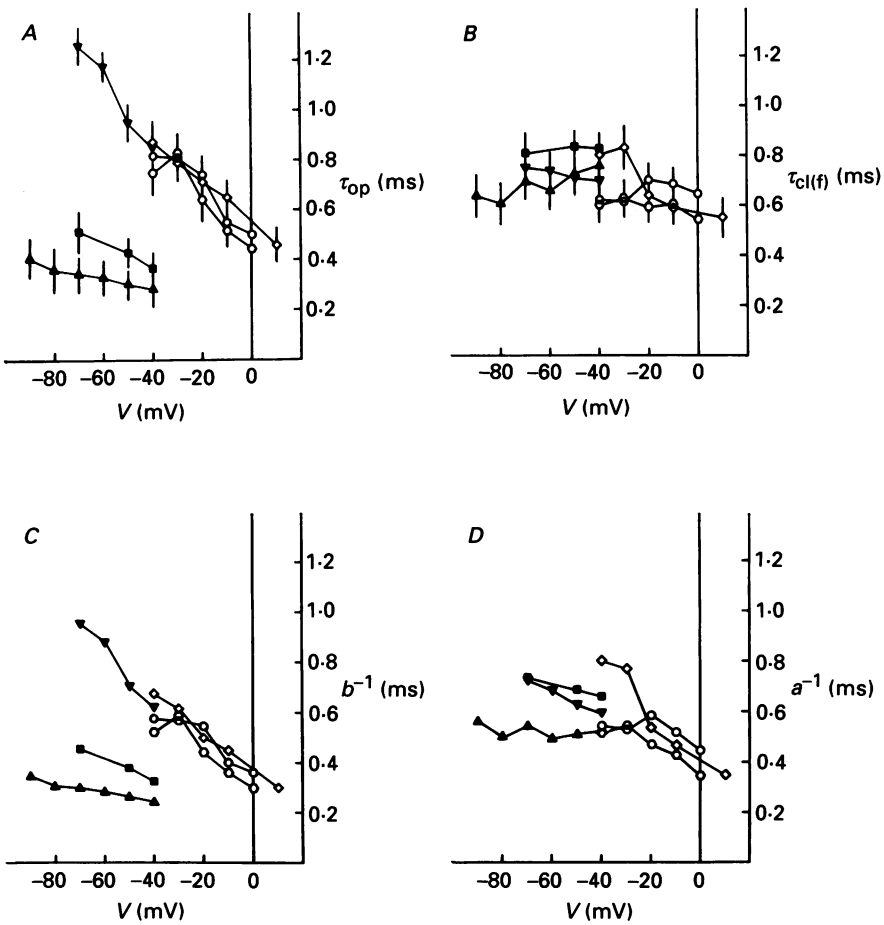

Fig. 8. Potential dependence of mean channel open time τ_{op} (*A*) and mean time of intraburst closures $\tau_{cl(f)}$ (*B*) for various permeant cations: ○, Ca^{2+}; ⬡, Sr^{2+}; ◇, Ba^{2+}; ▲, 100 mM-Na^+; ■, 40 mM-Na^+; ▼, 100 mM-Li^+. *C* and *D*, calculated values of inverse rate constants b^{-1} (*C*) and a^{-1} (*D*) for the same membrane potentials and charge carriers. Calculations were made after correction of τ_{op} and $\tau_{cl(f)}$ for missed events according to expressions (4) and (5) (see text). Each symbol indicates experimental values for at least three patches. Vertical bars, S.D. from the mean. All divalent charge carriers were 60 mM.

Since the time constants τ_{op} and $\tau_{cl(f)}$ are of relatively short duration missed events due to frequency limitations of the recording apparatus (2 kHz for Na^+-carried currents and 1 kHz for all others) could affect their numerical values. Using the results of Blatz & Magleby (1986) it is possible to show that if a, $b \gg \alpha$, β and $t_d \ll \tau_{op}$, $\tau_{cl(f)}$, (which are true for Ca^{2+} channels and our recording conditions), the

real channel open time T_{op} and the real time of intraburst gaps $T_{cl(f)}$ are related to the corresponding time τ_{op} and $\tau_{cl(f)}$ measured at a given bandwidth as follows:

$$1/b = T_{op} \simeq \tau_{op}(1-t_d/\tau_{cl(f)}), \quad (4)$$

$$1/(a+2\beta) = T_{cl(f)} \simeq \tau_{cl(f)}(1-t_d/\tau_{op}). \quad (5)$$

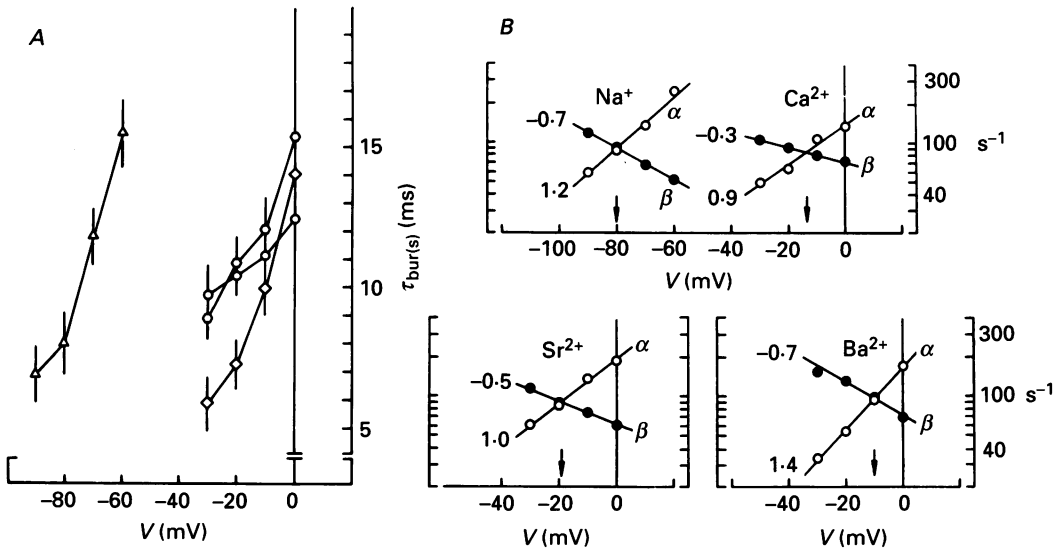

Fig. 9. Potential dependence of burst duration $\tau_{bur(s)}$ (A) and of rate constants α and β (B) for different charge carriers: ○, Ca^{2+}; ○, Sr^{2+}; ◇, Ba^{2+}; △, Na^{+} (all 60 mM). Straight lines in B are the best fit by eye to the experimental points. Corresponding semilogarithmic slopes are shown near each line. Arrows in B indicate intersection potentials of α- and β-lines.

The results of the definition of inverse rate constants b^{-1} and a^{-1} using corrected values of T_{op} and $T_{cl(f)}$ (below we shall use usual denotations, τ_{op} and $\tau_{cl(f)}$, implying corrected values) are given in Fig. 8C and D. One can note stronger dependence of b^{-1} compared to a^{-1} upon permeant ion species and concentration.

Burst duration for all charge carriers was found to be strongly potential dependent, increasing with depolarization. However, the steepness of $\tau_{bur(s)}(V)$ for various ions was not similar; it was weakest for Ca^{2+} and strongest for Ba^{2+} and Na^{+} (Fig. 9A). Figure 9B presents semilogarithmic plots of rate constants α and β. These rate constants define the character of activation curves for corresponding whole-cell currents. Experimental points could be satisfactory fitted with the straight lines indicating exponential dependence of rate constants α and β on membrane potential. The intersection points between the α- and β-lines correspond to the membrane potentials of half-activation of the channel. The observed shifts of $V_{\frac{1}{2}}$ in response to substitution of charge carriers are in good agreement with those obtained from I–V relations for whole-cell currents (Fig. 1) and activation curves (Fig. 3C).

Semilogarithmic slopes of α and β for various charge carriers are different. As the initial two kinetic stages in model (1) can formally be related to the intramembrane

transfer of two charged gating particles, the slope of ln $\alpha(V)/\beta(V)$ represents the effective valency of each m-particle (m is an activation variable). Hence it is possible to conclude that this value is noticeably affected by permeant ion species.

DISCUSSION

Identification of Ca^{2+} channel type

The data obtained confirm our suggestion that the Ca^{2+} channels in undifferentiated neuroblastoma cells most resemble the LTI (T-type) Ca^{2+} channels in other preparations. These channels are similar in their macroscopic kinetics and selectivity properties and are practically independent of the intercellular metabolic support. Shifts of Ca^{2+} channel potential-dependent characteristics in neuroblastoma cell membrane caused by substitution of permeant divalent cations are also quite similar to those for LTI channels (e.g. Fukushima & Hagiwara, 1985).

Ca^{2+} channel selectivity

Ca^{2+} channel permeability is known to be determined by the depth of energy wells representing ion binding sites (for review see Tsien, Hess, McCleskey & Rosenberg, 1987) and by the height of the potential barrier which in general depends on electrostatic interaction of the permeant ion with the anionic groups of the selectivity filter, and sterical correspondence of hydrated ion to its pore (Hille, 1975). Since LTI Ca^{2+} channel conductance in our experiments was found to be identical for Ca^{2+}, Sr^{2+} and Ba^{2+} it is possible to suppose that the affinities of these ions to channel binding sites and the height of the potential barriers for them are also quite similar.

Permeability of the channel for monovalent cations depends mainly upon the sterical factors. Recently, based on the fact that the largest organic cation able to permeate through the modified HTN (or L-type) Ca^{2+} channel was tetramethylammonium (TMA), a circle of 0·6 nm in diameter was proposed for its sterical part (McCleskey & Almers, 1985; Tsien *et al.* 1987). However, noticeable permeability of TMA through the LTI Ca^{2+} channels in lymphocytes has not been detected (Fukushima & Hagiwara, 1985). We are inclined to the idea that the dimensions of the sterical regions for Ca^{2+} channels of different types are similar and are close to those for Na^+ channel (0·3 × 0·5 nm (Hille, 1975)). Indeed, all Ca^{2+} channels after modification of their selectivity can pass almost the same monovalent cations as Na^+ channels (Kostyuk *et al.* 1983; Fukushima & Hagiwara, 1985; McCleskey & Almers, 1985). Some peculiarities of the selectivity properties may be explained by different flexibility of sterical regions. If so, then for some channels the size of the pore of the selectivity filter may not exactly correspond to the diameter of the largest permeable ion. Additional arguments in favour of this idea come from structural homology of Na^+ and Ca^{2+} channels (Miller, 1989).

The effect of permeant ions on mean channel open time

The data obtained show that permeant ion type and concentration can noticeably affect the mean Ca^{2+} channel open time, τ_{op}, which characterizes the rate of Ca^{2+} channel transition from open (O) into nearest closed state (A). This suggests that channel closure is probably due to sterical narrowing of the selectivity filter.

Recently, it was shown by Läuger (1985) that ions which occupy channel binding site(s) can affect the rate constants of conformation transitions accompanying channel gating due to electrostatic interaction with the polar groups of channel protein. Although we consider such an 'electrostatic mechanism' important, the difference in the ion dependence of the inverse rate constants a^{-1} and b^{-1} cannot be explained by this mechanism alone. In our opinion to account for the stronger ion dependence of b^{-1} which characterizes the mean channel open time not only static, but also dynamic interaction of the permeating ion with polar molecular groups of Ca^{2+} channel selectivity filter should be considered.

Such interaction may occur if the hydrated ion passing through the open Ca^{2+} channel does not sterically correspond to the cross-section of the selectivity filter. In this case the local displacements, δ_i, of charged molecular groups and consequently the system of dipoles, $e\delta_i$ ($e = 1{\cdot}6 \times 10^{-19}$ C), may occur along the ion trajectory. The mean induced dipole moment will depend on the relation between the ion permeation rate and the rate of dipole relaxation, which for proteins is of the order of 10^7 s^{-1} (Burfoot & Taylor, 1979). According to Debye's theory the mean dipole moment determines the effective dielectric constant for a system of weakly interacting molecular groups (Burfoot & Taylor, 1979). Thus, in the presence of ionic flux one might expect increased dielectric constant, ϵ_i, of the channel sterical region compared to the value $\epsilon_0 \simeq 3$ which is characteristic for static proteins (Honig, Hubbel & Flewelling, 1986). This, in turn, will result in a decrease in part of the transmembrane electric field falling on this region and governing the stage of channel conformational closure. Such a process may be detected as a decrease in the potential dependence of the mean channel open time.

Since the real dimensions of the pore of the LTI Ca^{2+} channel selectivity filter (as well as of other channels) are unknown it is difficult to make quantitative estimates related to this mechanism. However, we have found that at relatively high Na^+ concentrations when $g_{Na} \simeq 60$ pS the rate of Na^+ ion transfer through the channel starts to approach the rate of dipole relaxation. For such conditions it is sufficient to suppose a local displacement, δ_{Na}, of only 0·016 nm to obtain the increase in the dielectric constant of the channel sterical region from ϵ_0 up to $\epsilon_{Na} \simeq 30$. Divalent charge carriers and Na^+ ions at low $[Na^+]_o$ due to the decrease of ion permeation rate are able to increase the dielectric constant of the sterical region by about 10% at maximum compared to its static value. Finally, Li^+ ions, as the smallest, may not induce any dipole moment ($\delta_{Li} = 0$) and the dielectric constant of the sterical region in the presence of Li^+ flux will not increase at all ($\epsilon_{Li} = \epsilon_0$). Figure 8*C* shows that the potential dependence of τ_{op} ($\tau_{op} = b^{-1}$) reasonably reflects expected changes of the dielectrical constant produced by different ions. This potential dependence is highest for Li^+, decreases for divalent charge carriers and Na^+ at low concentrations, and almost disappears for high $[Na^+]_o$; in parallel shortening of τ_{op} occurs.

The proposed mechanism for the ion dependence of τ_{op} is consistent with previous observations on Ca^{2+} channels from rat brain synaptosomes (Nelson, 1986). For these Ca^{2+} channels (probably high threshold), the mean open time was found to be shortest for Ba^{2+} ions which had the highest permeation rate (and biggest ionic radius), and it increased in parallel with the decrease of single-channel conductance (and ionic radius) for Sr^{2+}, Ca^{2+} and Mn^+.

When studying the activation kinetics of single LTI Ca^{2+} channels in monovalent ion conducting mode we kept the external Ca^{2+} concentration at 10^{-8} M which is low enough to exclude specific blocking action of Ca^{2+} ions. We expect that increasing $[Ca^{2+}]_o$ will lead to the appearance of blocking events resulting in the reduction of mean channel open time as was found by Lux, Carbone & Zucker (1988) on LTI Ca^{2+} channels from chick DRG neurons. In this preparation τ_{op} for sodium current was halved at $[Ca^{2+}]_o \simeq 5 \times 10^{-5}$ M.

The effect of permeant ions on the channel closed states

After channel transition from the open state (O) to the nearest closed state (A) the sterical region becomes narrow and ion flux through the channel is no longer possible. That is why the inverse rate constant a^{-1} which characterizes the backward transition to an open state is less ion-dependent than b^{-1}.

Variation in the permeant ion type causes changes in the logarithmic slopes of $\alpha(V)$ and $\beta(V)$ and shifts of the half-activation potential of the channel. These effects can be explained by supposing that Ca^{2+} channel binding sites have a geometrical arrangement along the pathway of gating charge transfer. In this case, consistent with the 'electrostatic mechanism' proposed by Läuger (1985), the energies of the states R and C will include the component describing electrostatic interaction between the bound cation and the gating charge. A high-affinity binding site in the Ca^{2+} channel outer mouth responsible for selectivity modification (Kostyuk *et al.* 1983) can add much to such interaction if the initial localization of charged gating particles in the channel resting state (R) is in a close proximity to this binding site. The 70 mV hyperpolarizing shift of the activation curve for the modified Ca^{2+} channel, which is much larger than the possible shift due to an increase in surface potential in the absence of divalent cations ($V_s = -30$ mV; Mironov & Dolgaya, 1987), indicates that this might be the case.

Contribution of inactivation

The Ca^{2+} channels in neuroblastoma cells as well as LTI Ca^{2+} channels in other preparations are relatively fast-inactivating in a voltage-dependent manner (Bean, 1985; Fedulova *et al.* 1985; Carbone & Lux, 1987*a*). According to our data, the time constant (τ_{in}) of Sr^{2+} current decay during sustained depolarization to 0 mV is 17 ms (not shown). Since theoretically the LTI Ca^{2+} channel can enter the inactive state (I) from each state of the activation process (Carbone & Lux, 1987*b*; Droogmans & Nilius, 1989) all rate constants measured in the present investigation can be influenced by inactivation and this influence needs to be assessed.

First, inactivation results in the appearance of additional exponential components in the closed time histograms having time constants bigger than $\tau_{cl(f)}$, $\tau_{cl(s)}$ and $\tau_{cl(vs)}$. In fact, we observed some 'extra slow tails' in these histograms. However, due to the relative infrequency of events contributing to these 'tails' and due to their contamination by false closings (see Methods), an adequate description was impossible. In determining the rate constant α, first latency histograms were used and these are minimally affected by inactivation. In contrast, mean burst duration can be strongly affected by inactivation due to channel transition from state A into inactive state I. Thus, the apparent difference in potential dependence of $\tau_{bur(s)}$ and

slopes of β (Fig. 9) can partially be attributed to the effect of various ions on channel inactivation. Indeed, some difference in inactivation time course of Ca^{2+}, Sr^{2+} and Ba^{2+} whole-cell currents can be noted in Fig. 1*A*. Slowing of inactivation of the LTI Ba^{2+} current compared to the Ca^{2+} current in the DRG neurons was also detected by Carbone & Lux (1987*a*).

Consideration of the additional transition of the channel from open state O into inactive state I due to the big difference between τ_{op} and τ_{in} may change the rate constant b defining channel conformational closure by not more than 2%. Thus, this rate constant can be considered inversely proportional to τ_{op} without introducing a significant error.

The authors wish to thank Professor P. G. Kostyuk for helpful discussions and a critical reading of the manuscript and Professor T. F. McDonald (Halifax, Canada) and Dr D. Pelzer (Homburg/Saar, Germany) for the review of its final version.

REFERENCES

ALMERS, W., MCCLESKEY, E. W. & PALADE, P. T. (1984). A non-selective cation conductance in frog muscle membrane blocked by micromolar external calcium ions. *Journal of Physiology* **353**, 565–583.

ASHCROFT, F. M. & STANFIELD, P. R. (1981). Calcium dependence of the inactivation of calcium currents in skeletal muscle fibres of an insect. *Science* **213**, 224–226.

BEAN, B. P. (1985). Two kinds of calcium channels in canine atrial cells. Differences in kinetics, selectivity, and pharmacology. *Journal of General Physiology* **86**, 1–30.

BLATZ, A. L. & MAGLEBY, K. L. (1986). Correcting single channel data for missed events. *Biophysical Journal* **49**, 967–980.

BOSSU, J. L., FELTZ, A. & THOMANN, J. M. (1985). Depolarization elicits two distinct calcium currents in vertebrate sensory neurons. *Pflügers Archiv* **403**, 360–368.

BROWN, A. M., MORIMOTO, K., TSUDA, Y. & WILSON, D. L. (1981). Calcium current-dependent and voltage-dependent inactivation of calcium channels in *Helix aspersa*. *Journal of Physiology* **320**, 193–218.

BROWN, A. M., TSUDA, Y. & WILSON, D. L. (1983). A description of activation and conduction in calcium channels based on tail and turn-on current measurements in the snail. *Journal of Physiology* **344**, 549–583.

BURFOOT, J. C. & TAYLOR, G. W. (1979). *Polar Dielectrics and their Applications*. Macmillan Press, New York.

BYERLY, L. & HAGIWARA, S. (1982). Calcium currents in internally perfused nerve cell bodies of *Limnea stagnalis*. *Journal of Physiology* **322**, 503–528.

CARBONE, E. & LUX, H. D. (1984). A low voltage-activated, fully inactivating Ca channel in vertebrate sensory neurones. *Nature* **310**, 501–503.

CARBONE, E. & LUX, H. D. (1987*a*). Kinetics and selectivity of a low-voltage-activated calcium current in chick and rat sensory neurones. *Journal of Physiology* **386**, 547–570.

CARBONE, E. & LUX, H. D. (1987*b*). Single low-voltage-activated calcium channels in chick and rat sensory neurones. *Journal of Physiology* **386**, 571–601.

CARBONE, E. & LUX, H. D. (1988). Sodium currents through neuronal calcium channels: kinetics and sensitivity to calcium antagonists. In *The Calcium Channel: Structure, Function and Implications*, ed. MORAD, M., NAYLER, W., KAZDA, S. & SCHRAMM, M., pp. 115–127. Springer-Verlag, Berlin, Heidelberg, New York, London. Paris, Tokyo.

CAVALIE, A., OCHI, R., PELZER, D. & TRAUTWEIN, W. (1983). Elementary currents through Ca^{2+} channels in guinea pig myocytes. *Pflügers Archiv* **398**, 284–297.

CHAD, J. E. & ECKERT, R. (1986). An enzymatic mechanism for calcium current inactivation in dialysed *Helix* neurones. *Journal of Physiology* **378**, 31–51.

COLQUHOUN, D. & SIGWORTH, F. J. (1983). Fitting and statistical analysis of single channel recordings. In *Single Channel Recording*, ed. SAKMANN, B. & NEHER, E., pp. 191–263. Plenum Press, New York.

DROOGMANS, G. & NILIUS, B. (1989). Kinetic properties of the cardiac T-type calcium channel in the guinea-pig. *Journal of Physiology* **419**, 627–650.

DURROUX, T., GALLO-PAYET, N. & PAYET, M. D. (1988). Three components of the calcium current in cultured glomerulosa cells from rat adrenal gland. *Journal of Physiology* **404**, 713–729.

ECKERT, R. & TILLOTSON, D. L. (1981). Calcium-mediated inactivation of the calcium conductance in caesium-loaded giant neurones of *Aplysia californica*. *Journal of Physiology* **314**, 265–280.

FEDULOVA, S. A., KOSTYUK, P. G. & VESELOVSKY, N. S. (1985). Two types of calcium channels in the somatic membrane of new-born rat dorsal root ganglion neurons. *Journal of Physiology* **359**, 431–446.

FENWICK, E. M., MARTY, A. & NEHER, E. (1982). Sodium and calcium channels in bovine chromaffin cells. *Journal of Physiology* **331**, 599–635.

FISHMAN, M. C. & SPECTOR, I. (1981). Potassium current suppression by quinidine reveals additional calcium currents in neuroblastoma cells. *Proceedings of the National Academy of Sciences of the USA* **78**, 5245–5249.

FOX, A. P., NOWYCKY, M. C. & TSIEN, R. W. (1987*a*). Kinetic and pharmacological properties distinguishing three types of calcium currents in chick sensory neurones. *Journal of Physiology* **394**, 149–172.

FOX, A. P., NOWYCKY, M. C. & TSIEN, R. W. (1987*b*). Single-channel recordings of three types of calcium channels in chick sensory neurones. *Journal of Physiology* **394**, 173–200.

FUKUSHIMA, Y. & HAGIWARA, S. (1985). Currents carried by monovalent cations through calcium channels in mouse neoplastic B lymphocytes. *Journal of Physiology* **358**, 255–284.

GANITKEVICH, V., SHUBA, M. F. & SMIRNOV, S. V. (1987). Calcium-dependent inactivation of potential-dependent calcium inward current in an isolated guinea-pig smooth muscle cell. *Journal of Physiology* **392**, 431–449.

HAGIWARA, S., OZAWA, S. & SAND, O. (1975). Voltage clamp analysis of two inward current mechanisms in the egg cell membrane of a starfish. *Journal of General Physiology* **65**, 617–644.

HAMILL, O. P., MARTY, A., NEHER, E., SAKMANN, B. & SIGWORTH, F. (1981). Improved patch-clamp techniques for high-resolution current recording from cells and cell-free membrane patches. *Pflügers Archiv* **391**, 85–100.

HESS, P., LANSMAN, J. B. & TSIEN, R. W. (1986). Calcium channel selectivity for divalent and monovalent cations. *Journal of General Physiology* **88**, 293–319.

HILLE, B. (1975). Ionic selectivity of Na and K channels of nerve membranes. In *Lipid Bilayers and Biological Membranes: Dynamic Properties*, ed. EISENMAN, G., pp. 255–323. Marcel Dekker, New York.

HONIG, B. H., HUBBEL, W. L. & FLEWELLING, R. W. (1986). Electrostatic interactions in membranes and proteins. *Annual Review of Biophysics and Biophysical Chemistry* **15**, 163–193.

KOSTYUK, P., AKAIKE, N., OSIPCHUK, YU., SAVCHENKO, A. & SHUBA, YA. (1989*a*). Gating and permeation of different types of Ca channels. *Annals of the New York Academy of Sciences* **560**, 63–79.

KOSTYUK, P. G., KRISHTAL, O. A. & SHAKHOVALOV, YU. A. (1977). Separation of sodium and calcium currents in the somatic membrane of mollusc neurones. *Journal of Physiology* **270**, 545–568.

KOSTYUK, P. G., MIRONOV, S. L. & SHUBA, YA. M. (1983). Two ion-selecting filters in the calcium channel of the somatic membrane of mollusc neurons. *Journal of Membrane Biology* **76**, 83–93.

KOSTYUK, P. G. & SHIROKOV, R. E. (1989). Deactivation kinetics of different components of calcium inward current in the membrane of mice sensory neurones. *Journal of Physiology* **409**, 343–355.

KOSTYUK, P. G., SHUBA, YA. M. & SAVCHENKO, A. N. (1988*a*). Three types of calcium channels in the membrane of mouse sensory neurons. *Pflügers Archiv* **411**, 661–669.

KOSTYUK, P. G., SHUBA, YA. M., SAVCHENKO, A. N. & TESLENKO, V. I. (1988*b*). Kinetic characteristics of different calcium channels in neuronal membrane. In *The Calcium Channel: Structure, Function and Implications*, ed. MORAD, M., NAYLER, W., KAZDA, S. & SCHRAMM, M., pp. 442–464. Springer-Verlag, Berlin, Heidelberg, New York, London, Paris, Tokyo.

KOSTYUK, P. G., SHUBA, YA. M. & TESLENKO, V. I. (1989*b*). Activation kinetics of single high-threshold calcium channels in the membrane of sensory neurons from mouse embryos. *Journal of Membrane Biology* **110**, 29–38.

LÄUGER, P. (1985). Ionic channels with conformational substates. *Biophysical Journal* **47**, 581–591.

LUX, H. D., CARBONE, T. & ZUCKER, H. (1988). Block of sodium currents through a neuronal calcium channel by external calcium and magnesium ions. In *The Calcium Channel: Structure, Function and Implications*, ed. MORAD, M., NAYLER, W., KAZDA, S. & SCHRAMM, M., pp. 128–137. Springer-Verlag, Berlin, Heidelberg, New York, London, Paris, Tokyo.

MCCLESKEY, E. W. & ALMERS, W. (1985). The Ca channel in skeletal muscle is a large pore. *Proceedings of the National Academy of Sciences of the USA* **82**, 7149–7153.

MCDONALD, T. F., CAVALIE, A., TRAUTWEIN, W. & PELZER, D. (1986). Voltage-dependent properties of macroscopic and elementary calcium channel currents in guinea pig ventricular myocytes. *Pflügers Archiv* **406**, 437–448.

MAGLEBY, K. L. & PALLOTA, B. S. (1983). Burst kinetics of single calcium-activated potassium channels in cultured rat muscle. *Journal of Physiology* **344**, 605–673.

MATTESON, D. R. & ARMSTRONG, C. M. (1986). Properties of two types of calcium channels in clonal pituitary cells. *Journal of General Physiology* **87**, 161–182.

MILLER, C. (1989). Genetic manipulation of ion channels: a new approach to structure and mechanism. *Neuron* **2**, 1195–1205.

MIRONOV, S. L. & DOLGAYA, E. V. (1987). 1041-Microelectrophoresis and fluorescence studies of the glicoprotein sheath covering the outer membrane surface in murine neuroblastoma cells. *Biochemistry and Bioenergetics* **17**, 429–439.

MOOLENAAR, W. H. & SPECTOR, I. (1978). Ionic currents in cultured mouse neuroblastoma cells under voltage-clamp conditions. *Journal of Physiology* **278**, 265–286.

NARAHASHI, T., TSUNOO, A. & YOSHII, M. (1987). Characterization of two types of calcium channels in mouse neuroblastoma cells. *Journal of Physiology* **383**, 231–249.

NELSON, M. T. (1986). Interactions of divalent cations with single calcium channels from rat brain synaptosomes. *Journal of General Physiology* **87**, 201–222.

NOWYCKY, M. C., FOX, A. P. & TSIEN, R. W. (1985). Three types of neuronal calcium channel with different calcium agonist sensitivity. *Nature* **316**, 440–443.

QUANDT, F. N. & NARAHASHI, T. (1984). Isolation and kinetic analysis of inward currents in neuroblastoma cells. *Neuroscience* **13**, 249–262.

SAIMI, Y. & KUNG, C. (1982). Are ions involved in the gating of calcium channels? *Science* **218**, 153–156.

SHUBA, YA. M. & TESLENKO, V. I. (1987). Kinetic model for activation of single calcium channels in mammalian sensory neurone membrane. *Biological Membranes (Moscow)* **4**, 315–329.

TILLOTSON, D. (1979). Inactivation of Ca conductance dependent on entry of Ca ions in molluscan neurons. *Proceedings of the National Academy of Sciences of the USA* **76**, 1497–1500.

TSIEN, R. W., HESS, P., MCCLESKEY, E. W. & ROSENBERG, R. L. (1987). Calcium channels: mechanism of selectivity, permeation and block. *Annual Review of Biophysics and Biophysical Chemistry* **16**, 265–290.

VESELOVSKY, N. S. & FEDULOVA, S. A. (1983). Two types of calcium channels in the somatic membrane of rat dorsal root ganglion neurons. *Doklady Akademii Nauk SSSR (Moscow)* **268**, 747–756.